DR AYŞEGÜL DOĞAN (Orcid ID : 0000-0003-4160-2270)

Article type : Research Article

Design and Synthesis of Phenylpiperazine Derivatives as Potent Anticancer Agents for Prostate Cancer

Serpil Demirci[1], Taha Bartu Hayal[2], Binnur Kıratlı[2], Hatice Burcu Şişli[2], Selami Demirci[3], Fikrettin Sahin[2], Ayşegül Doğan[2*]*

[1]Giresun University, Vocational High School of Health Services, Department of Medical Services and Techniques, Giresun, Turkey

[2]Yeditepe University, Department of Genetics and Bioengineering, Faculty of Engineering, Istanbul, Turkey

[3]National Heart, Lung, and Blood Institute (NHLBI), Sickle Cell Branch, Cellular and Molecular Therapeutics National Institutes of Health (NIH)

Running title: Phenylpiperazine Derivatives as Anticancer Agents

Acknowledgments

The support provided by Scientific and Technological Research Council of Turkey (TUBITAK, Project no: 116Z932) is gratefully acknowledged.

Authors do not have any conflict of interest

ABSTRACT

Novel thiourea (**5a**, **5b**) and thiazolidinone derivatives (**6a**, **6b**) were synthesized by hybridizing molecules starting from the compound 6-(4-phenyl-piperazin-1-yl)pyridine-3-ylamine (**4**) which is known to show anticancer activity. The synthesis of the leading compound was carried out by using 1-

(5-nitropyridin-2-yl)-4-phenylpiperazine (**3**) which was obtained by a novel method of the reaction of 2-chloro-5-nitropyridine (**1**) and N-phenylpiperazine (**2**). The structures of the compounds were confirmed using FT IR, ^{1}H NMR, ^{13}C NMR, HRMS spectroscopic methods and elemental analysis. The organic molecules were tested for their anticancer activities against prostate cancer cell lines; DU 145, PC-3 and LNCaP. As the compound **5a** exerted the highest cytotoxic activity, IC_{50} concentrations of **5a** were further investigated in terms of morphology, colony forming ability, RNA expression, fragmented DNA and cell cycle distributions of prostate cancer cell lines. Overall data revealed that **5a** treatment induces apoptosis and DNA fragmentation in prostate cancer cell lines and inhibits cell cycle progression resulting in the accumulation of cells in either the G1 or S phases.

Keywords: Antitumor activity, apoptosis, cell cycle, DNA fragmentation, thiourea, thiazolidinone

INTRODUCTION

Prostate cancer (PC) is the leading noncutaneous cancer type among men in US with an expected 174,650 new cases and 31,620 deaths in 2019. PC is the second lethal cancer with a 10% mortality ratio after lung cancer (24%) (Siegel, Miller, & Jemal, 2019). As a multistep and complicated cancer type, PC progression is regulated by androgen activity at the cellular level which is the basis of hormone deprivation therapy at early stages when PC cells are still responsive to androgen suppression. (Gregory et al., 2001) While prostatectomy followed by radiation therapy is the standard therapy in clinics for early diagnosed cases (Sriprasad, Feneley, & Thompson, 2009), patients with advanced stage disease remain incurable due to resistance to chemotherapy, acquired androgen-refractory phenotype, and inefficient radiation therapies (Jarvis, Nelius, Martinez□Marin, Sennoune, & Filleur, 2018; Oudard, 2013; Seruga, Ocana, & Tannock, 2011). Treatment at late stage of PC could only be possible by combining surgical removal, radiotherapy and chemotherapy options based on clinical priority to monitor adverse outcomes (Nicolae, Venugopal, & Ravi, 2016; Teply & Hauke, 2016). Although heterogenous nature of PC restricts the treatment, chemotherapy is generally considered as a prior treatment regimen with both adjuvant and neo-adjuvant options (Beer & Raghavan, 2000). Combination of different chemotherapeutic agents is a new therapeutic modality but still remains insufficient for improved life expectancy and quality, a goal that is demanding for current clinical trials (Demirci et al., 2017). Therefore, development of novel chemotherapeutics displaying targeted cytotoxicity to PC cells is still focus of international research.

Substantial advances in the technology and synthetic chemistry coupled with traditional methodology is expected to enable identification of various novel drug molecules in near future. In this manner, combinatorial chemistry based on the use of building blocks, scaffolds and libraries of standard chemical reactions, in solid or solution phases by simple addition and incubation steps, has an important role in the synthesis of small organic compounds. Of those organic compounds, thiourea derivatives, used as precursors for the synthesis of different classes of biologically active acyclic and heterocyclic compounds, have recently gained importance thanks to their broad biological activities such as anti-inflammatory, antimicrobial, antimalarial and pesticidal functions (Ghorab et al., 2016). Additional biochemical and pharmacological studies have confirmed that these molecules are also effective against various cancer cell lines including breast cancer (Lv, Li, Sun, Zhou, & Zhu, 2010), nasopharyngeal carcinoma (Peng et al., 2011), lung and liver cancer cell lines (Hu et al., 2017) through mainly inhibiting receptor tyrosine kinases (RTKs), protein tyrosine kinases (PTKs), and DNA topoisomerases (Kumar & Chimni, 2015).

Thiazolidinone derivatives, another group of biologically active organic compounds which have different substituents around the core nucleus, are also considered as potential anticancer agents. Their strong affinity for various biological targets including JNK-stimulating phosphatase-1 (JSP-1) (Cutshall, O'Day, & Prezhdo, 2005), non-membrane protein tyrosine phosphatase (SHP-2) (Geronikaki et al., 2008), tumour necrosis factor-α (Carter et al., 2001), and antiapoptotic biocomplex Bcl-xL/BH3 (Degterev et al., 2001) might be potential reasons for the anticancer activity. Anti-cancer activities for various thiazolidinone compounds against breast cancer (Wu et al., 2014), glioblastoma (Avdieiev et al., 2014) and drug resistant lung cancer (Zhou et al., 2008) have been reported in the literature.

Here we synthesized and characterized novel thiourea and thiazolidinone derivatives as anti-cancer agents. The anticancer activities of the compounds were evaluated against PC cell lines. Cancer cells treated with the highest activity displaying compound, **5a**, were examined in terms of cell morphology, RNA expression profile, DNA fragmentation and cell cycle distribution to explore possible action of mechanism of the organic molecule.

EXPERIMENTAL SECTION

1. Chemistry

1.1. General Methods

All chemicals were purchased from FlukaChemie AG Buchs (Switzerland). Melting points of the synthesized compounds were determined in open capillaries on a Buchi B-540 melting point apparatus and are uncorrected. Reactions were monitored by thin-layer chromatography (TLC) on

0.25 mm silicagel plates (GF254) and visualized under UV light. FT IR spectra were recorded using a Mattson 1000 FT-IR spectrometer. ^{1}H NMR and ^{13}C NMR spectra were recorded on Bruker Avene II 400 MHz NMR spectrometer (chemical shift in ppm downfield from TMS as an internal reference). The elemental analysis was performed on a Leco CHNS-932 (Michigan, USA) elemental analyzer. The mass spectra were obtained at a high-resolution mass spectra (HRMS) TOF (1200/6210, Agilent) by electrospray ionization.

1.2. 1-(5-Nitropyridin-2-yl)-4-phenylpiperazine (3)

2-Chloro-4-nitropyridine (**1**) (0.63 g, 4 mmol) was added dropwise to *N*-phenylpiperazine (**2**) (1.62 g, 10 mmol) at 0-5 °C over 20 min. The temperature was gradually raised to 135 °C and refluxed for 4h. The reaction was cooled at room temperature and water was added. The enthusiast was filtered in the fridge overnight. Crystallization with EtOAc-hexane gave a pale brown product. Yield, 60% (1.68 g); mp, 155-156 °C; **^{1}H-NMR (400 MHz, $CDCl_3$):** δ 9.06 (d, 1H, *J*: 2.7 Hz), 8.23 (dd, 1H, *J*: 9.5, 2.7 Hz), 7.32-7.27 (m, 2H), 6.96-6.90 (m, 3H), 6.61 (d, 1H, *J*: 9.5 Hz), 3.94 (d, 4H, *J*: 5.14 Hz), 3.42 (d, 4H, *J*: 5.14 Hz); **APT (^{13}C-NMR) (100 MHz, DMSO-d_6):** δ 165.30,155.80, 151.29, 139.59, 138.08, 134.23, 124.46, 120.86, 110.92, 53.44, 49.49; **FT IR (cm^{-1}):** 3072 (ar-CH), 1593-1290 (NO_2); **Elemental analysis for** $C_{15}H_{16}N_4O_2$ calculated; C, 63.37; H, 5.67; N, 19.71; found: C, 63.28; H, 5.85; N, 19.75; **HRMS (APCI):** *m/z* calculated: $C_{15}H_{16}N_4O_2$ (M^+ + H): 285.32; found: 285.13.

1.3. 6-(4-Phenylpiperazin-1-yl)pyridin-3-amine (4)

Compound (**3**) (2.85 g, 10 mmol) was refluxed by the addition of Pd/C (0.53 g, 5 mmol) in a two necked flask and stirring in n-butanol in an oil bath. After the reflux started, 60% hydrazine hydrate (2.5 g, 4.04 ml, 50 mmol) was added dropwise over 20 min. It was refluxed for 15 h. At the end of the time the hot reaction mixture was filtered through the celite. The solvent was removed by evaporation. Crystallization with EtOAc-hexane gave a dark red product. Yield, 95% (2.41 g); mp,136-137 °C; **^{1}H-NMR (400 MHz, DMSO-d_6):** δ 7.64 (d, 1H, *J*: 2.7 Hz), 7.23 (t, 2H, *J*: 7.8 Hz), 7.00-6.94 (m, 3H), 6.80 (t, 1H, *J*: 7.21 Hz), 6.70 (d, 1H, *J*: 8.76 Hz), 4.59 (s, 2H, NH_2), 3.36-3.49 (m, 4H), 3.26-3.16 (m, 4H); **APT (^{13}C-NMR) (100 MHz, DMSO-d_6):** δ 151.34,134.92, 134.72, 129.16, 126.48, 120.00, 116.39, 116.37, 108.86, 49.29, 46.91; **FT IR (cm^{-1}):** 3309 and 3201 (NH_2), 3008 (ar-CH); **Elemental analysis for** $C_{17}H_{16}O_2$ calculated: C, 70.84; H, 7.13; N, 22.03, found: C, 70.49; H, 7.27; N, 21.99; **HRMS (APCI):** *m/z* calculated: $C_{15}H_{18}N_4$ (M^+ + H): 255.34; found: 255.15.

1.4. General Method for the Synthesis of Compounds 5a, 5b

Phenylisothiocyanate (for **5a**) (10 mmol), benzylisothiocyanate (for **5b**) (10 mmol) were added to the solution of compound **4** (10 mmol) in a dried DCM drop-wise and the mixture was refluxed for 8-18h. The solid precipitate was collected by filtration and recrystallized from suitable solvent to afford the desired compound.

1-Phenyl-3-(6-(4-phenylpiperazin-1-yl)pyridin-3-yl)thiourea (5a)

Crystallized EtOAc; dark pink solid product. Yield 51% (1.95 g); mp, 144-145 °C; **^{1}H-NMR (400 MHz, DMSO-d_6):** δ 9.72 (s, 1H, NH), 9.49 (s, 1H, NH), 8.09 (d,1H, *J*: 2.5 Hz), 7.62 (dd, 1H, *J*: 8.9, 2.5 Hz),7.48 (d, 2H, *J*: 8.1 Hz), 7.33 (t, 2H, *J*: 7.8 Hz), 7.25 (t, 2H, *J*: 7.9 Hz), 7.13 (t, 1H, *J*: 7.4 Hz), 7.01 (d, 2H, *J*: 8.2 Hz), 6.90 (d, 1H, *J*: 9.0 Hz), 6.81 (t, 1H, *J*: 7.2 Hz), 3.65-3.62 (m, 4H), 3.26-3.23 (m, 4H); **APT (^{13}C-NMR) (100 MHz, DMSO-d_6):** δ 181.25, 157.29, 151.71, 145.05, 140.10, 136.34, 129.68, 129.16, 127.36, 125.15, 124.47, 119.89, 116,45, 107.29, 48.89, 45.63; **FT IR (KBr,cm^{-1}):** 3199 (NH), 3023 (ar-CH), 1227 (C=S); **Elemental analysis for** $C_{22}H_{23}N_5S$ calculated: C, 67.84; H, 5.95; N, 17.98; S: 8.23, found: C, 67.89; H, 5.91; N, 17.89; S, 7.98; **HRMS (APCI):** *m/z* calculated: $C_{22}H_{23}N_5S$ (M^+ + H): 390.52; found: 390.42.

1-Benzyl-3-(6-(4-phenylpiperazin-1-yl)pyridin-3-yl)thiourea (5b)

Crystallized EtOAc; dark green solid product. Yield 85% (3.43 g); mp, 139-140 °C; **^{1}H-NMR (400 MHz, DMSO-d_6):** δ 9.35 (s,1H, NH), 8.06 (bs, 2H, arH+NH), 7.55 (d, 1H, *J*: 8.8 Hz), 7.34-7.32 (m, 4H), 7.24 (t, 3H, *J*: 8 Hz), 7.0 (d, 2H, *J*: 8.1 Hz), 6.90 (d, 1H, *J*: 9.0 Hz), 6.81 (t, 1H, *J*: 7.2 Hz), 4.72 (d, 2H, *J*: 4.5 Hz), 3.63 (d, 4H, *J*: 4.0 Hz), 3.23 (d, 4H, *J*: 4.3 Hz); **APT (^{13}C-NMR)(100 MHz, DMSO-d_6):** δ 182.41, 157.16, 151.47, 144.93, 139.69, 136.16, 129.45, 128.69, 127.80, 127.25, 126.51, 119.64, 116.21, 107.35, 48.66, 47.80, 45.36; **FT IR (cm^{-1}):** 3258, 3181 (2NH), 3028 (ar-CH), 1226 (C=S); **Elemental analysis for** $C_{23}H_{25}N_5S$ calculated: C, 68.46; H, 6.24; N, 17.35; S, 7.95, found: C: 68.43, H: 6.27, N: 17.67, S: 7.62; **HRMS (APCI):** *m/z* calculated: $C_{23}H_{25}N_5S$ (M^+ + H): 404.55; found: 404.19.

1.5. General Method for the Synthesis of Compounds 6a, 6b

A mixture of compound **5a** (for **6a**), **5b** (for **6b**) (10 mmol) and ethyl bromoacetate (10 mmol) in absolute ethanol allowed to reflux in the presence of dried sodium acetate (50 mmol) for 15-18 h. The reaction mixture was then cooled to room temperature. After the solvent was removed under reduced pressure. Then water was added to the solution that led to solid structure formation. This crude product was recrystallized from a suitable solvent to afford the desired compound.

3-Phenyl-2-((6-(4-phenylpiperazin-1-yl)pyridin-3-yl)imino)thiazolidin-5-one (6a)

Crystallized EtOAc; light brown solid product. Yield %53 (2.27 g); mp, 163 °C; **^{1}H-NMR (400 MHz, $CDCl_3$):** δ 8.22 (d, 1H, *J*: 2.5 Hz) 7.52 (dd, 1H, *J*: 9.0, 2.6 Hz), 7.33-7.27 (m, 4H), 7.12 (t, 1H, *J*: 7.4 Hz),6.97 (d, 2H, *J*: 7.4 Hz), 6.92-6.87 (m, 3H), 6.78 (d, 1H), 3.98 (s,2H), 3.77 (t, 4H, *J*: 5.2 Hz), 3.29 (t, 4H, *J*: 5.2 Hz); **APT (^{13}C-NMR) (100 MHz, DMSO-d_6):** δ 172.25, 158.59, 156.50, 151.43, 148.58, 147.39, 137.98,129.71, 129.45, 124.67, 122.39, 121.14, 119.65, 116.23, 107.35, 48.64, 45.03, 33.20; **FT IR (cm^{-1}):** 3023 (ar-CH), 1729 (C=O); **Elemental analysis for** $C_{24}H_{23}N_5OS$ calculated: C, 67.11; H: 5.40; N, 16.30; S, 7.46, found: C, 67.78; H, 5.36; N, 15.96; S, 7.20; **HRMS (APCI):** *m/z* calculated $C_{24}H_{23}N_5OS$ (M^+ + H): 430.54; found: 430.15.

3-Benzyl-2-((6-(4-phenylpiperazin-1-yl)pyridin-3-yl)imino)thiazolidin-5-one (6b)

Crystallized EtOAc; light yellow solid product. Yield 93% (4.43 g); mp, 140-141 °C; **^{1}H-NMR (400 MHz, DMSO-d_6):** δ 7.83 (s, 1H),7.36-7.32 (m, 4H), 7.29-7.23 (m, 4H), 6.99 (d, 2H, *J*: 8.0 Hz), 6.91 (d, 1H, *J*:8.8 Hz), 6.80 (t, 1H, *J*: 6.8 Hz), 4.92 (bs, 2H), 4.12 (s, 2H), 3.60 (bs, 4H), 3.23 (bs, 4H); **APT (^{13}C-NMR)(100 MHz, DMSO-d_6):** δ 172,37, 156.83, 155.73, 151.47, 140.31, 136.66, 135.51, 131.37, 129.44, 128.90, 128.21, 127.91, 119.61, 116.19,107.92, 48.63, 45.92, 45.49, 33.07; **FT IR (cm^{-1}):** 3014 (ar-CH), 1721 (C=O), 1619 (C=N); **Elemental analysis for** $C_{25}H_{25}N_5OS$ calculated: C, 67.70; H, 5.68; N, 15.79; S, 7.23 found: C, 67.64; H, 5.84; N, 15.62; S, 7.31; **HRMS (APCI):** *m/z* $C_{25}H_{25}N_5OS$ calculated (M^+ + H): 444.57; found: 444.19.

2. Anticancer Activity

2.1. Cell lines and proliferation assay

Human prostate cancer cell lines, PC-3 (CRL-1435), DU 145 (HTB-81), and LNCaP (CRL-1740), were purchased from ATCC (Rockville, Maryland, USA). All cell lines were incubated in Dulbecco`s Modified Eagle Media (DMEM, Invitrogen) supplemented with 10% fetal bovine serum (FBS, Invitrogen) and 1% penicillin-streptomycin-amphotericin (PSA, Invitrogen) in a humidified incubator at 37°C and 5% CO_2 conditions. Anticancer activity of newly synthesized hybrid molecules against prostate cancer cell lines were assessed with 3- (4,5-dimethylthiazol-2-yl)-2,5-diphenyl-tetrazolium bromide (MTT) assay and NCI60 response parameters was used at the end of 24h incubation period. Results are given as % cell inhibition. Optic density for the cells treated only with solvent (DMSO) was accepted as 100%. Reponse parameters, IC_{50} (50% cell viability inhibition), GI_{50} (50% growth inhibition), TGI (total growth inhibition), and LC_{50} (50% cell death) were anayzed based on National Institutes of Health (NIH) definitions using logaritmic fonctions (González-Vallinas et al., 2013).

2.2. Colony-forming Unit (CFU) Assay

CFU assay was performed to determine whether compound **5a** affects the colony-forming ability of cells as described previously (Demirci et al., 2018). Briefly, PC-3, DU145 and LNCaP cells were seeded at a cell density of 100 cell per well of 6-well plates in the presence of respective IC_{50} concentrations of **5a** for each cell line. Media were replaced with growth medium after 24h compound 5a treatment. Cells were incubated for an additional 13 days at 37 °C in a humidified incubator. Colonies were stained with crystal violet, counted and imaged with Zeiss PrimoVert light microscope with an AxioCam ERc5 s camera and Zen 2011 software (Carl Zeiss Microscopy, LLC, Thornwood, NY, USA).

2.3. Morphological Analyses: light microscope

Cell morphology was determined by light microscope analysis after **5a** exposure for 24 h. Briefly, 10^5 cells/well were seeded onto 12 well plates and exposured to IC_{50} concentrations of **5a**. Apoptotic morphology was determined by images taken after 24 h using Zeiss PrimoVert light microscope with an AxioCam ERc5 s camera and Zen 2011 software (Carl Zeiss Microscopy, LLC, Thornwood, NY, USA).

2.4. Quantitative RT-PCR (q-PCR) analysis

q-PCR experiments were performed according to the previously described protocol (Doğan, Demirci, Apdik, Apdik, & Şahin, 2017). Primers for p21, MDM2, Caspase-3, Caspase-7, AKT, PI3K and GAPDH were designed using Primer-BLAST software from the National Center for Biotechnology (Bethesda,MD, USA) and synthesized by Macrogen (Seoul, Korea). GAPDH was used as housekeeping gene. Total RNA from **5a** treated PC-3, DU145 and LNCaP cells were isolated using RNAeasy plus mini kit (Qiagen, Hilden, Germany) and cDNA was synthesized using High Fidelity cDNA synthesis kit (Roche, USA). q-PCR analyses performed by using SYBR method and CFX96 RT-PCR system (Bio-Rad, Hercules, CA).

2.5. DNA Fragmentation

DNA fragmentation, as an indicator of DNA damage and apoptosis, was performed according to the previously described protocol (Ji et al., 2012). In short, cells were seeded onto 6 well plates (Corning Plasticware, Corning, NY) at a cell density of 3×10^5 cells/well. Cells were treated with compound **5a** for 24h. DNA was isolated from **5a** treated cells by using DNA isolation kit (Invitrogen, USA). DNA samples were loaded to 1% agarose gel in Tris-borate buffer, stained with ethidium bromide (EtBr, Sigma, USA) and images were obtained using the luminometer system (Bio-Rad).

2.6. Cell Cycle Analysis

The cell cycle distribution of PC-3, DU145 and LNCaP cells after **5a** treatment was measured using propidium iodide (PI) staining. Cells were fixed with 70% cold ethanol and incubated with 1 ml PI staining solution containing 40 µg/ml PI, 10 µg/ml RNase A, and 0.1% NP-40 for 30 min at 37 °C. Cell cycle analyses were performed using a Becton Dickinson FACSCalibur flow cytometry system (Becton Dickinson, San Jose, CA, USA).

2.7. ADMET Analysis

In silico ADME study, which is one of the computational calculations, was applied for the synthesized compounds. In this study, we calculated molecular volume (MV), molecular weight (MW), logarithm of partition coefficient (miLogP), number of hydrogen bond acceptors (n-ON), number of hydrogen bonds donors (n-OHNH), topological polar surface area (TPSA), number of rotatable bonds (n-ROTB) and Lipinski's rule of five using Molinspiration online property calculation toolkit (Molinspiration Cheminformatics, Bratislava, Slovak Republic, http://www.molinspiration.com/cgi-bin/properties). Absorption (% ABS) was calculated by: % ABS = 109 − (0.345xTPSA) (Y. H. Zhao et al., 2002).

2.8. Statistical Analysis. The data were statistically analyzed using one-way analysis of variance. The values of $p \leq 0.05$ were considered statistically significant.

RESULTS AND DISCUSSION

Chemistry

The synthetic strategies adapted to obtain the target compounds are depicted in **Scheme 1**. To obtain 6-(4-phenylpiperazin-1-yl)pyridin-3-amine (**4**), which is also a commercially available organic molecule, previously published protocol was followed (Walsh, Sneddon, & Moody, 2013). However, we could not be able to synthesize the 1-(5-Nitropyridin-2-yl)-4-phenylpiperazine (**3**) molecule using the same methodoloy. Unlike the proposed protocol, we presented an optimal synthesis method for the organic molecule, which was performed in a solvent-free environment in an oil bath. Spectroscopic data for the compound **3** have been shown for the first time (see **Suplementary file 1**).

Synthesis of thiourea derivatives (**5a, 5b**) were accomplished by nucleophilic attack of the amine compound (**4**) to the alkylisothiocyanates (**Scheme 1**). In the FT IR spectra, the signals originated from –C=S function of compounds **5a** and **5b** appeared between 1226-1227 cm^{-1}. In the ^{13}C NMR spectra of these compounds (**5a, 5b**), –C=S function resonated between 182.41-181.25 ppm (see **Suplementary file 1**). Further evidence for the formation of carbothioamides was the presence of four –NH- signals at 9.72– 8.06 ppm in the ^{1}H NMR spectra. The elemental analysis data of carbon, hydrogen and nitrogen were formed to be satisfactory and within the permissible limit error.

Reaction and conditions for the synthesis of compounds **3-6**. *i*: 2-Chloro-4-nitropyridine in acetonitrile, 4 h, ruflux; *ii*: $H_2NNH_2.H_2O$ in But-OH, Pd/C, 15 h, ruflux; *iii*: Phenylisothiocyanate (for **5a**) or benzylisothiocyanate (for **5b**) in DCM, 8 h, ruflux; *iv*: ethyl bromoacetate, dry CH_3COONa in absolute ethanol, 13-15 h, ruflux.

Synthesis of thiazolidinone derivatives (**6a, 6b**) were carried out starting from intermediates of thiourea (**5a, 5b**). Compounds (**6a, 6b**) were characterized by the presence of additional strong band at 1729-1721 cm^{-1} in the FT IR spectrum corresponding to additional carbonyl function which arose from ring-closure. This was considered as a confirmation of thiazolidinone nucleus formation. Moreover, ^{1}H NMR, ^{13}C NMR spectrums, the elemental analyses and mass spectral data were compatible with the suggested structure (see **Suplementary file 1**).

ADMET Prediction

All synthesized compounds exhibited a good % ABS (91.05-94.02%) based on all parameters (**Table 1**). It was monitored that none of the com-pound violated Lipinski's rule of five (Table 1). It can be suggested that these two compounds may be developed as good drug candidates. A molecule probably to be evolved as an orally active drug candidate should exhibit no more than one violation of the following four criteria: logP (octanole − water partition coefficient) ≤5, molecular weight ≤500, number of hydrogen bond acceptors ≤10 and number ofhydrogen bond donors ≤5 (Ertl, Rohde, & Selzer, 2000). Since the obtained compounds (5a and 6a) followed this rule for orally active drug and therefore can be promoted as oral drug candidates.

Compound 5a contains thiosemicarbazone group and compound 6a is a thiazolidinone derivative. Thiosemicarbazone derivatives has been reported for their anticancer activities in the literature (Altıntop et al., 2016). Similarly, thiazolidinone derivatives such as Ciglitazone, Rosiglitazone, Pioglitazone demonstrated anti-cancer activity (Chinthala et al., 2013). The study has demonstrated the synthesis of some novel 1-(5-nitropyridin-2-yl)-4-phenylpiperazine (**3**) derivatives with anticancer activities by incorporating several pharmacophore groups such as structures of phenylisothiocyanate, benzisothiocyanate and thiazolidinone rings.

Anticancer activity

5a Reduces the Cell Proliferation Rate And CFU Ability of PC Cells.

After characterization of the molecules, possible GI_{50}, TGI, LC_{50} and IC_{50} levels were determined against PC cell lines. **Table 2** shows that the thiourea and thiazolidinone derivatives displayed growth inhibitory effects against PC cell lines comparable to 5-fluorouracil which is a validated anticancer drug against several solid tumors (Longley, Harkin, & Johnston, 2003).

While GI_{50} levels of all organic molecules remained at low concentrations (3.34-64.49 μM for DU 145, 4.62-74.66 μM for PC-3 and 4.71-279.14 μM for LNCaP), LC_{50} and TGI concentrations were higher than 500 μM (the highest concentration tested) for most of the compunds. IC_{50} levels, used as a clinically relevant concentration to determine the potency of a given drug, were mostly over the test range for thiazolidnone derivatives while concentrations for thiourea compounds were comparable to 5-FU (102.95-175.35 μM for DU 145, 14.90-160.41μM for PC-3 and 301.13->500 μM for LNCaP (**Table 2**). The thiourea derivatives (**5a** and **5b**) exhibited robust inhibitory activity against DU 145 and PC-3 but they remained relatively weak against LNCaP. LnCaP is an androgen responsive cell line, but the canonical androgen pathway does not work for PC-3 and DU145 cells (Marchiani et al., 2010), indicating that thiourea derivatives might target a different proliferation pathway other than the androgen pathway. As **5a** was more effective against PC cell lines compared to compound **5b**, we selected **5a** for further action of mechanism studies.

To further evaluate the viability effect of **5a**, PC cells were treated with respective IC_{50} concentrations of the organic molecule for 24 h and CFU abilities were investigated after a 14-days incubation period. CFU capacity of PC-3 and DU 145 cells were not significantly affected by **5a** treatment, while colonies become irregular and smaller in size, showing anti-proliferative effect of the compound rather than affecting colony formation capacity (**Figure 1**).

On the other hand, CFUs in LNCaP cells exposed to **5a** significantly reduced, which is consistent with the proliferation assay showing a different mechanism of inhibitory action on androgen-responsive and unresponsive cells.

5a Treatment Diminishes Cancer Cell Growth by Inducing Apoptosis and DNA Damage.

PC cell lines were tested for RNA expression profile and morphology to see whether the **5a** treatment triggers apoptotic pathway. Incubation with **5a** lead to apoptotic cell formation in PC-3 and DU 145 cells (**Figure 2A**). In line with this, live cell imaging confirmed high prevalence of apoptotic cancer cells treated with the compound during the culture period (**Supplementary video 1, 2, and 3**). Having this finding, to propose a possible mechanism, q-PCR assay was conducted to analyze apoptosis-related RNA levels in PC cells. The results revealed that caspase-3 was induced in all three cells, while there was a slight change in caspase-7, proposing that apoptosis might be executed through caspase-3 dependent pathway (**Figure 2B**). Apoptosis induction using various approaches is one of the leading ways of current clinical practice to cope with cancers. In this manner, cancer progression or metastasis are controlled either introducing apoptotic intermediate enhancing factors such as reactive oxygen species (Redza-Dutordoir & Averill-Bates, 2016) or decreasing the levels of anti-apoptotic proteins such as Bcl-2, Bcl-X_L, and Bcl-w (Sarosiek & Letai, 2016). Thus, apoptosis induction in all cells treated with **5a** would be promising, if it is proven safe and effective in animal models.

PI3K/AKT pathway manages several cell responses including cell cycle progression, survival, proliferation and activates protein biosynthesis (Xia & Xu, 2015). It has been stated that almost every major components of the pathway is mutated in a large variety of solid tumors resulting in permanent activation of AKT (Carnero & Paramio, 2014). As expected AKT levels were lower in **5a** treated PC cells that might be the possible explanation for survival inhibitory activity (**Figure 2B**). In normal cells, PTEN is upstream element of the pathway, inhibiting the activation of AKT (Carnero, Blanco-Aparicio, Renner, Link, & Leal, 2008). Given the fact that while DU 145 cells express functional PTEN, PC-3 cells are PTEN-null and LNCaP cells do not have active PTEN (Jäntti et al., 2018), downregulation of AKT would have been PTEN-independent way. Correspondingly, inherited and spontaneous tumors with PTEN deficiency or loss has been presented (Cantley & Neel, 1999), suggesting that AKT activation can also be in the absence of PTEN or in the presence of an PTEN analog. Likewise, integrin-linked kinase (ILK) 1-associated AKT phosphorylation was reported in PC-3 and LNCaP cells (Persad et al., 2000). Although q-PCR results propose that apoptotic pathway is triggered, and the survival pathway is inhibited by **5a** treatment, additional protein studies are needed to validate this observation and explore the exact inhibitory mechanism**.**

To evaluate whether the apoptotic activity is related with DNA damaging activity of the organic molecule, we conducted DNA fragmentation assay for **5a** treated PC cells (**Figure 3**). The results confirmed that although control cells also have DNA fragmentation, **5a** treatment augmented DNA breaks. To address if this is an indirect effect or direct interaction of the compound with DNA, additional interaction experiments should be performed.

5a Inhibits Cell Cycle Progress.

5a exposed cells were subjected to flow cytometry analysis to evaluate possible cell cycle dysregulation. **Figure 4** demonstrates that there is an increase of cells in the S phase and a corresponding decrease of cells in the G2/M phases in **5a** treated PC-3 and DU 145 cells. The reason for S phase arrest is most likely due to the inhibitory action of thiourea derivatives on DNA topoisomers (Esteves-Souza, Pissinate, da Graça Nascimento, Grynberg, & Echevarria, 2006; Y. Zhao, Wang, Wu, Fang, & Zhu, 2012) that overwind or underwind of DNA during replication. This observation also explains antiproliferative effect of **5a** treatment on PC-3 and DU 145 cells as CFU results showed same colony numbers in treated and control groups but smaller colonies **5a** treated cells. On the other hand, **5a** treatment resulted in G1 arrest in LNCaP cells which is in line with the hypothesis that cytotoxic effect of 5**a** on these cells is through different mechanisms.

CONCLUSION

This study reports synthesis of some new 1-(5-nitropyridin-2-yl)-4-phenylpiperazine (**3**) derivatives by incorporating several biologically important heterocyclic moieties; phenylisothiocyanate,

benzisothiocyanate and thiazolidinone rings. The structures of new compounds were confirmed by FT IR, ^{1}H-, ^{13}C NMR, mass spectroscopic and elemental analysis techniques. These organic molecules were tested for their anticancer activities against androgen-responsive and unresponsive PC cell lines. Thiourea derivatives exhibited higher cytotoxicity; and of those, **5a** was found to be the highest anticancer activity displaying organic molecule. Molecular mechanism analysis revealed that **5a** exerted its activity through induction of DNA damage, apoptosis and cell cycle arrest. This study highlights the importance of novelthiourea derivative **5a,** as a potential anti-cancer agent to improve PC chemotherapy by inducing apoptosis. Further studies are required to explore its exact action of mechanism that may allow us to elucidate functional groups' roles in the anticancer activity. Moreover, this organic molecule might be modified to specifically target cancer cells for clinical perspective. Combination with known anticancer agents to increase clinical benefits would be another option for chemothraphy resistant cancer types.

Acknowledgments

The support provided by Scientific and Technological Research Council of Turkey (TUBITAK, Project no: 116Z932) is gratefully acknowledged.
Research data are not shared.

Conflict of Interest

Authors do not have any conflict of interest.

AUTHOR INFORMATION

Corresponding Authors

*E-mail: aguldgn@gmail.com (A. Doğan); demirciserpil17@gmail.com (S. Demirci).

TBH provided and cultured cancer cells and conducted prolideraion analyses, BK and HBŞ conducted all remaining *in vitro* experiments, FŞ and SD helped analyzing the data. Serpil Demirci synthyzed and characterized the chemicals. Serpil Demirci and Ayşegül Doğan designed the experimens and organized as a manuscript.

ORCID

Ayşegül Doğan: 0000-0003-4160-2270; Serpil Demirci: 0000-0002-6579-4273

SUPPLEMENTARY MATERİAL

Supplementary File. ^{1} H- and ^{13}C-NMR spectra of each reference compound.

Supplementary Video 1. Live imaging for DU 145 cells treated with **5a**

Supplementary Video 2. Live imaging for PC-3 cells treated with **5a**

Supplementary Video 3. Live imaging for LNCaP cells treated with **5a**

ABBREVIATIONS USED

FT IR, Fourier transform infrared spectroscopy; KBr, potassium bromide; ^{1}H NMR, proton nuclear magnetic resonance; ^{13}C NMR, carbon nuclear magnetic resonance; APT, Attached proton test; HRMS, high-resolution mass spectrometry; TLC, thin-layer chromatography; TMS, tetramethylsilane; DNA, deoxyribonucleic acid; RNA, ribonucleic acid; IC_{50}, half-maximum inhibitory concentration; PC, Prostate cancer; RTKs, receptor tyrosine kinases; PTKs, protein tyrosine kinases; JSP-1, JNK-stimulating phosphatase-1; SHP-2, non-membrane protein tyrosine phosphatase; DMSO-d_6, deuterated dimethyl sulfoxide; $CDCl_3$, deuterated chloroform; Pd/C, palladium on carbon; EtOAc, ethyl acetate; DCM, dichloromethane; $H_2NNH_2.H_2O$, hydrazine hydrate; CH_3COONa, sodium acetate; s, singlet; d, doublet; dd, doublet of doublets; m, multiplet; t, triplet; MTT, 3-(4,5-dimethylthiazol-2-yl)-2,5-diphenyl-tetrazolium bromide; DMEM, dulbecco`s modified eagle media; FBS, fetal bovine serum; PSA, penicillin-streptomycin-amphotericin; GI_{50}, 50% growth inhibition; TGI, total growth inhibition; LC_{50}, 50% cell death; NIH, National Institutes of Health; CFU, colony-forming unit; q-PCR, Quantitative RT-PCR.

Figure Legends

Figure 1: Effect of compund **5a** on colony formation ability of cancer cell lines. Colony-forming capacity of PC-3, DU145 and LNCaP cells were demonstrated in comparison with 5-Fluorouracil (5-FU). Colonies were stained with crystal violet and counted. The numbers of colonies were significantly low only in LNCaP cells. The diameters of colonies were small in compund 5a treated cancer cell lines which was shown in colony morphology images. Notes: * $p<0.05$, Scale bar: 100 µm, 5-FU: 5-Fluorouracil.

Figure 2: Morphological observation of apoptotis and gene expression analyses of apoptotic/proliferative pathway genes. (A) Light microscope analyses of 24h compund **5a** treated PC-3, DU 145 and LNCaP. Apoptotic cells with round morphology were observed after 24 h exposure in both compund 5a and 5-Fluorouracil (5-FU) treated groups. (B) Gene expression analyses of compund **5a** treated PC-3, DU 145 and LNCaP cells. Expression of apoptotic/proliferative genes exerted a diverse pattern in three different cell types indicating the potential cell type spesific action. Notes: Scale bar: 200µm, 5-FU: 5-Fluorouracil.

Figure 3: Effect of compund **5a** on DNA fragmentation. Compund 5a and 5-Fluorouracil (5-FU) treatment induced DNA damage in PC-3, DU145 and LNCaP cells which was detected by agrose DNA gel electrophoresis. DNA fragmentation was determined by 1.0% agarose gel electrophoresis of genomic DNA isolated from Compund 5a and 5-FU treated prostate cancer cell lines. Notes: 5-FU: 5-Fluorouracil.

Figure 4: Effect of compund **5a** treatment on cell cycle progression in PC-3 (A), DU145 (B) and LNCaP (C) cells. Compund **5a** treatment resulted in cell accumalion at S phase for PC-3 and DU145 cells. In contrast, LNCaP cells were not able to pass through to the S and G2/M phases followed by compund **5a** treatment. Notes: 5-FU: 5-Fluorouracil.

REFERENCES

Altıntop, M. D., Atlı, Ö., Ilgın, S., Demirel, R., Özdemir, A., & Kaplancıklı, Z. A. (2016). Synthesis and biological evaluation of new naphthalene substituted thiosemicarbazone derivatives as potent antifungal and anticancer agents. *European journal of medicinal chemistry, 108*, 406-414.

Avdieiev, S., Gera, L., Havrylyuk, D., Hodges, R. S., Lesyk, R., Ribrag, V., . . . Kavsan, V. (2014). Bradykinin antagonists and thiazolidinone derivatives as new potential anti-cancer compounds. *Bioorganic & medicinal chemistry, 22*(15), 3815-3823.

Beer, T., & Raghavan, D. (2000). Chemotherapy for hormone□refractory prostate cancer: Beauty is in the eye of the beholder. *The Prostate, 45*(2), 184-193.

Cantley, L. C., & Neel, B. G. (1999). New insights into tumor suppression: PTEN suppresses tumor formation by restraining the phosphoinositide 3-kinase/AKT pathway. *Proceedings of the National Academy of Sciences, 96*(8), 4240-4245.

Carnero, A., Blanco-Aparicio, C., Renner, O., Link, W., & Leal, J. F. (2008). The PTEN/PI3K/AKT signalling pathway in cancer, therapeutic implications. *Current cancer drug targets, 8*(3), 187-198.

Carnero, A., & Paramio, J. M. (2014). The PTEN/PI3K/AKT pathway in vivo, cancer mouse models. *Frontiers in oncology, 4*, 252.

Carter, P. H., Scherle, P. A., Muckelbauer, J. A., Voss, M. E., Liu, R.-Q., Thompson, L. A., . . . Li, Z. (2001). Photochemically enhanced binding of small molecules to the tumor necrosis factor receptor-1 inhibits the binding of TNF-α. *Proceedings of the National Academy of Sciences, 98*(21), 11879-11884.

Chinthala, Y., Domatti, A. K., Sarfaraz, A., Singh, S. P., Arigari, N. K., Gupta, N., . . . Tiwari, A. K. (2013). Synthesis, biological evaluation and molecular modeling studies of some novel thiazolidinediones with triazole ring. *European journal of medicinal chemistry, 70*, 308-314.

Cutshall, N. S., O'Day, C., & Prezhdo, M. (2005). Rhodanine derivatives as inhibitors of JSP-1. *Bioorganic & medicinal chemistry letters, 15*(14), 3374-3379.

Degterev, A., Lugovskoy, A., Cardone, M., Mulley, B., Wagner, G., Mitchison, T., & Yuan, J. (2001). Identification of small-molecule inhibitors of interaction between the BH3 domain and Bcl-x L. *Nature cell biology, 3*(2), 173.

Demirci, S., Doğan, A., Apdik, H., Tuysuz, E. C., Gulluoglu, S., Bayrak, O. F., & Şahin, F. (2018). Cytoglobin inhibits migration through PI3K/AKT/mTOR pathway in fibroblast cells. *Molecular and cellular biochemistry, 437*(1-2), 133-142.

Demirci, S., Doğan, A., Türkmen, N. B., Telci, D., Rizvanov, A. A., & Şahin, F. (2017). Schiff base-Poloxamer P85 combination demonstrates chemotherapeutic effect on prostate cancer cells in vitro. *Biomedicine & Pharmacotherapy, 86*, 492-501.

Doğan, A., Demirci, S., Apdik, H., Apdik, E. A., & Şahin, F. (2017). Dental pulp stem cells (DPSCs) increase prostate cancer cell proliferation and migration under in vitro conditions. *Tissue and Cell, 49*(6), 711-718.

Ertl, P., Rohde, B., & Selzer, P. (2000). Fast calculation of molecular polar surface area as a sum of fragment-based contributions and its application to the prediction of drug transport properties. *Journal of medicinal chemistry, 43*(20), 3714-3717.

Esteves-Souza, A., Pissinate, K., da Graça Nascimento, M., Grynberg, N. F., & Echevarria, A. (2006). Synthesis, cytotoxicity, and DNA-topoisomerase inhibitory activity of new asymmetric ureas and thioureas. *Bioorganic & medicinal chemistry, 14*(2), 492-499.

Geronikaki, A., Eleftheriou, P., Vicini, P., Alam, I., Dixit, A., & Saxena, A. (2008). 2-Thiazolylimino/heteroarylimino-5-arylidene-4-thiazolidinones as new agents with SHP-2 inhibitory action. *Journal of medicinal chemistry, 51*(17), 5221-5228.

Ghorab, M. M., Alsaid, M. S., El-Gaby, M. S., Safwat, N. A., Elaasser, M. M., & Soliman, A. M. (2016). Biological evaluation of some new N-(2, 6-dimethoxypyrimidinyl) thioureido benzenesulfonamide derivatives as potential antimicrobial and anticancer agents. *European journal of medicinal chemistry, 124*, 299-310.

González-Vallinas, M., Molina, S., Vicente, G., de la Cueva, A., Vargas, T., Santoyo, S., . . . de Molina, A. R. (2013). Antitumor effect of 5-fluorouracil is enhanced by rosemary extract in both drug sensitive and resistant colon cancer cells. *Pharmacological research, 72*, 61-68.

Gregory, C. W., He, B., Johnson, R. T., Ford, O. H., Mohler, J. L., French, F. S., & Wilson, E. M. (2001). A mechanism for androgen receptor-mediated prostate cancer recurrence after androgen deprivation therapy. *Cancer research, 61*(11), 4315-4319.

Hu, H., Lin, C., Ao, M., Ji, Y., Tang, B., Zhou, X., . . . Wu, Z. (2017). Synthesis and biological evaluation of 1-(2-(adamantane-1-yl)-1 H-indol-5-yl)-3-substituted urea/thiourea derivatives as anticancer agents. *RSC Advances, 7*(81), 51640-51651.

Jäntti, M. H., Talman, V., Räsänen, K., Tarvainen, I., Koistinen, H., & Tuominen, R. K. (2018). Anticancer activity of the protein kinase C modulator HMI□1a3 in 2D and 3D cell culture models of androgen□responsive and androgen□unresponsive prostate cancer. *FEBS open bio, 8*(5), 817-828.

Jarvis, C., Nelius, T., Martinez□Marin, D., Sennoune, S. R., & Filleur, S. (2018). Cabazitaxel regimens inhibit the growth of prostate cancer cells and enhances the anti□tumor properties of PEDF with various efficacy and toxicity. *The Prostate*.

Ji, B.-C., Yu, C.-C., Yang, S.-T., Hsia, T.-C., Yang, J.-S., Lai, K.-C., . . . Chung, J.-G. (2012). Induction of DNA damage by deguelin is mediated through reducing DNA repair genes in human non-small cell lung cancer NCI-H460 cells. *Oncology reports, 27*(4), 959-964.

Kumar, V., & Chimni, S. S. (2015). Recent developments on thiourea based anticancer chemotherapeutics. *Anti-cancer agents in medicinal chemistry, 15*(2), 163-175.

Longley, D. B., Harkin, D. P., & Johnston, P. G. (2003). 5-fluorouracil: mechanisms of action and clinical strategies. *Nature reviews cancer, 3*(5), 330.

Lv, P.-C., Li, H.-Q., Sun, J., Zhou, Y., & Zhu, H.-L. (2010). Synthesis and biological evaluation of pyrazole derivatives containing thiourea skeleton as anticancer agents. *Bioorganic & medicinal chemistry, 18*(13), 4606-4614.

Marchiani, S., Tamburrino, L., Nesi, G., Paglierani, M., Gelmini, S., Orlando, C., . . . Baldi, E. (2010). Androgen□responsive and□unresponsive prostate cancer cell lines respond differently to stimuli inducing neuroendocrine differentiation. *International journal of andrology, 33*(6), 784-793.

Nicolae, A. M., Venugopal, N., & Ravi, A. (2016). Trends in targeted prostate brachytherapy: from multiparametric MRI to nanomolecular radiosensitizers. *Cancer nanotechnology, 7*(1), 6.

Oudard, S. (2013). Progress in emerging therapies for advanced prostate cancer. *Cancer treatment reviews, 39*(3), 275-289.

Peng, H., Liang, Y., Chen, L., Fu, L., Wang, H., & He, H. (2011). Efficient synthesis and biological evaluation of 1, 3-benzenedicarbonyl dithioureas. *Bioorganic & medicinal chemistry letters, 21*(4), 1102-1104.

Persad, S., Attwell, S., Gray, V., Delcommenne, M., Troussard, A., Sanghera, J., & Dedhar, S. (2000). Inhibition of integrin-linked kinase (ILK) suppresses activation of protein kinase B/Akt and induces cell cycle arrest and apoptosis of PTEN-mutant prostate cancer cells. *Proceedings of the National Academy of Sciences, 97*(7), 3207-3212.

Redza-Dutordoir, M., & Averill-Bates, D. A. (2016). Activation of apoptosis signalling pathways by reactive oxygen species. *Biochimica et Biophysica Acta (BBA)-Molecular Cell Research, 1863*(12), 2977-2992.

Sarosiek, K. A., & Letai, A. (2016). Directly targeting the mitochondrial pathway of apoptosis for cancer therapy using BH3 mimetics–recent successes, current challenges and future promise. *The FEBS journal, 283*(19), 3523-3533.

Seruga, B., Ocana, A., & Tannock, I. F. (2011). Drug resistance in metastatic castration-resistant prostate cancer. *Nature reviews Clinical oncology, 8*(1), 12.

Siegel, R. L., Miller, K. D., & Jemal, A. (2019). Cancer statistics, 2019. *CA: a cancer journal for clinicians, 69*(1), 7-34.

Sriprasad, S., Feneley, M. R., & Thompson, P. M. (2009). History of prostate cancer treatment. *Surgical oncology, 18*(3), 185-191.

Teply, B. A., & Hauke, R. J. (2016). Chemotherapy options in castration-resistant prostate cancer. *Indian journal of urology: IJU: journal of the Urological Society of India, 32*(4), 262.

Walsh, K., Sneddon, H. F., & Moody, C. J. (2013). Amination of Heteroaryl Chlorides: Palladium Catalysis or SNAr in Green Solvents? *ChemSusChem, 6*(8), 1455-1460.

Wu, J., Yu, L., Yang, F., Li, J., Wang, P., Zhou, W., . . . Yi, Z. (2014). Optimization of 2-(3-(arylalkyl amino carbonyl) phenyl)-3-(2-methoxyphenyl)-4-thiazolidinone derivatives as potent antitumor growth and metastasis agents. *European journal of medicinal chemistry, 80*, 340-351.

Xia, P., & Xu, X.-Y. (2015). PI3K/Akt/mTOR signaling pathway in cancer stem cells: from basic research to clinical application. *American journal of cancer research, 5*(5), 1602.

Zhao, Y., Wang, C., Wu, Z., Fang, J., & Zhu, L. (2012). Synthesis and antitumor activity of novel aroylthiourea derivatives of podophyllotoxin. *Investigational new drugs, 30*(1), 17-24.

Zhao, Y. H., Abraham, M. H., Le, J., Hersey, A., Luscombe, C. N., Beck, G., . . . Cooper, I. (2002). Rate-limited steps of human oral absorption and QSAR studies. *Pharmaceutical research, 19*(10), 1446-1457.

Zhou, H., Wu, S., Zhai, S., Liu, A., Sun, Y., Li, R., . . . Fang, B. (2008). Design, synthesis, cytoselective toxicity, structure–activity relationships, and pharmacophore of thiazolidinone derivatives targeting drug-resistant lung cancer cells. *Journal of medicinal chemistry, 51*(5), 1242-1251.

Table 1. Pharmacokinetic parameters important for good oral bioavailability of synthesized compound **5a** and **6**a.

Entry	% ABS	TPSA (A^2)	n-ROTB	MV	MW	miLog*P*	n-ON acceptors	n-OHNH donors	Nviolations
	-	-	-	-	≤500	≤5	<10	<5	≤1
5a	94.02	43.42	6	357.30	389.53	3.37	5	2	0
6a	91.05	52.04	4	383.75	429.55	4.87	6	0	0

% ABS: percentage absorption, TPSA: topological polar surface area, n-ROTB: number of rotatable bonds, MV: molecular volume, MW: molecular weight, miLog P: logarithm of partition coefficient of compound between n-octanol and water, n-ON acceptors: number of hydrogen bond acceptors, n-OHNH donors: number of hydrogen bonds donors.

Table 2. GI_{50}, TGI and LC_{50}) and IC_{50} values of the test molecules determined by MTT test

	DU145				**PC3**				**LnCaP**			
No	**GI_{50}**	**TGI**	**LC_{50}**	**IC_{50}**	**GI_{50}**	**TGI**	**LC_{50}**	**IC_{50}**	**GI_{50}**	**TGI**	**LC_{50}**	**IC_{50}**
3	17.23	>500	>500	>500	74.66	>500	>500	>500	79.14	>500	>500	>500
4	9.44	174.96	>500	175.35	18.48	160.41	>500	160.41	18.09	>500	>500	>500
5a	3.34	469.55	>500	102.95	4.62	15.40	>500	14.90	6.16	301.13	>500	301.13
5b	13.63	>500	>500	>500	21.06	>500	>500	>500	4.71	118.70	>500	85.99
6a	64.49	>500	>500	>500	15.60	>500	>500	>1000	13.50	>500	>500	>500
6b	45.76	>500	>500	>500	6.54	50.72	>500	36.75	13.07	>500	>500	>500

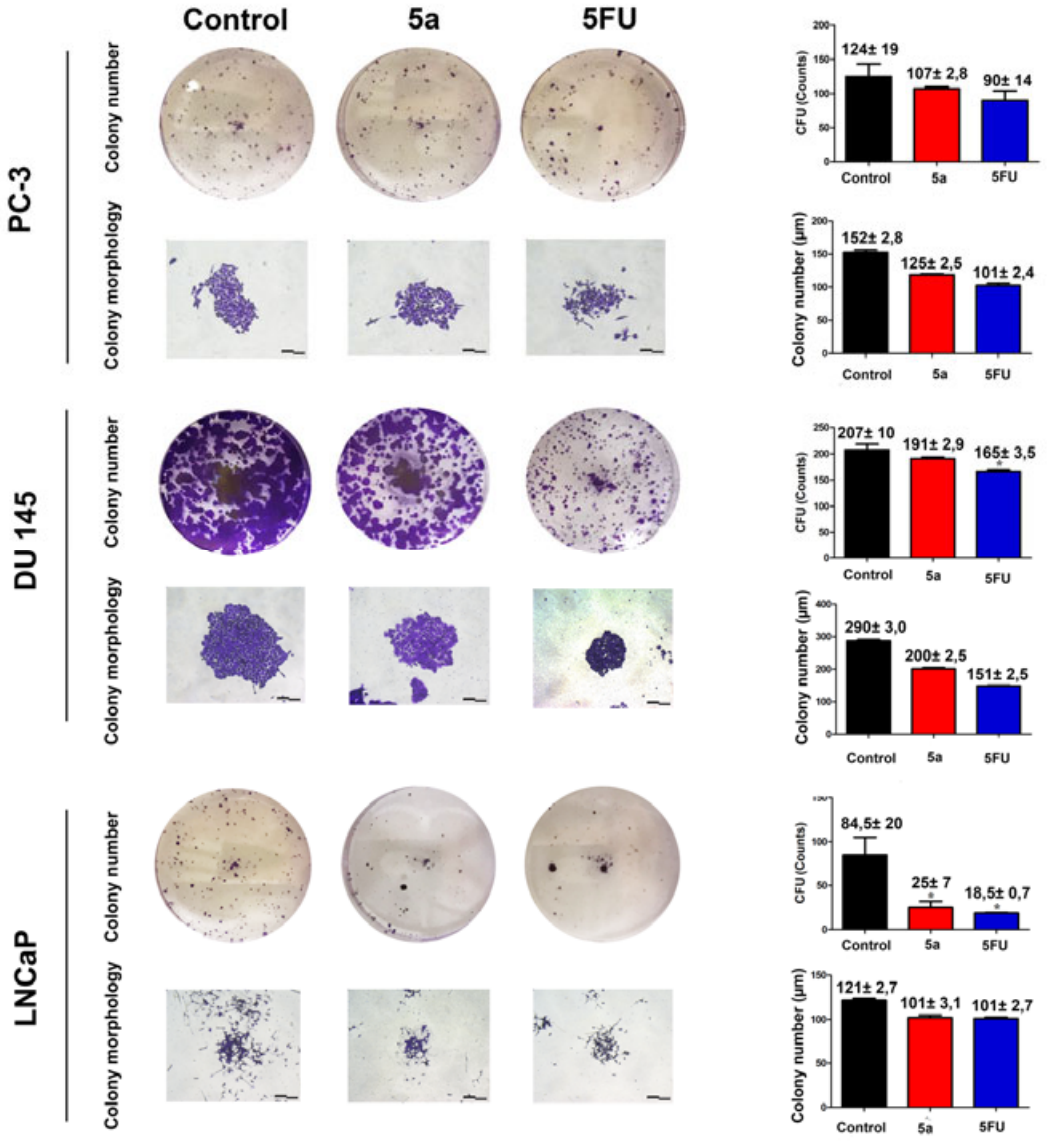

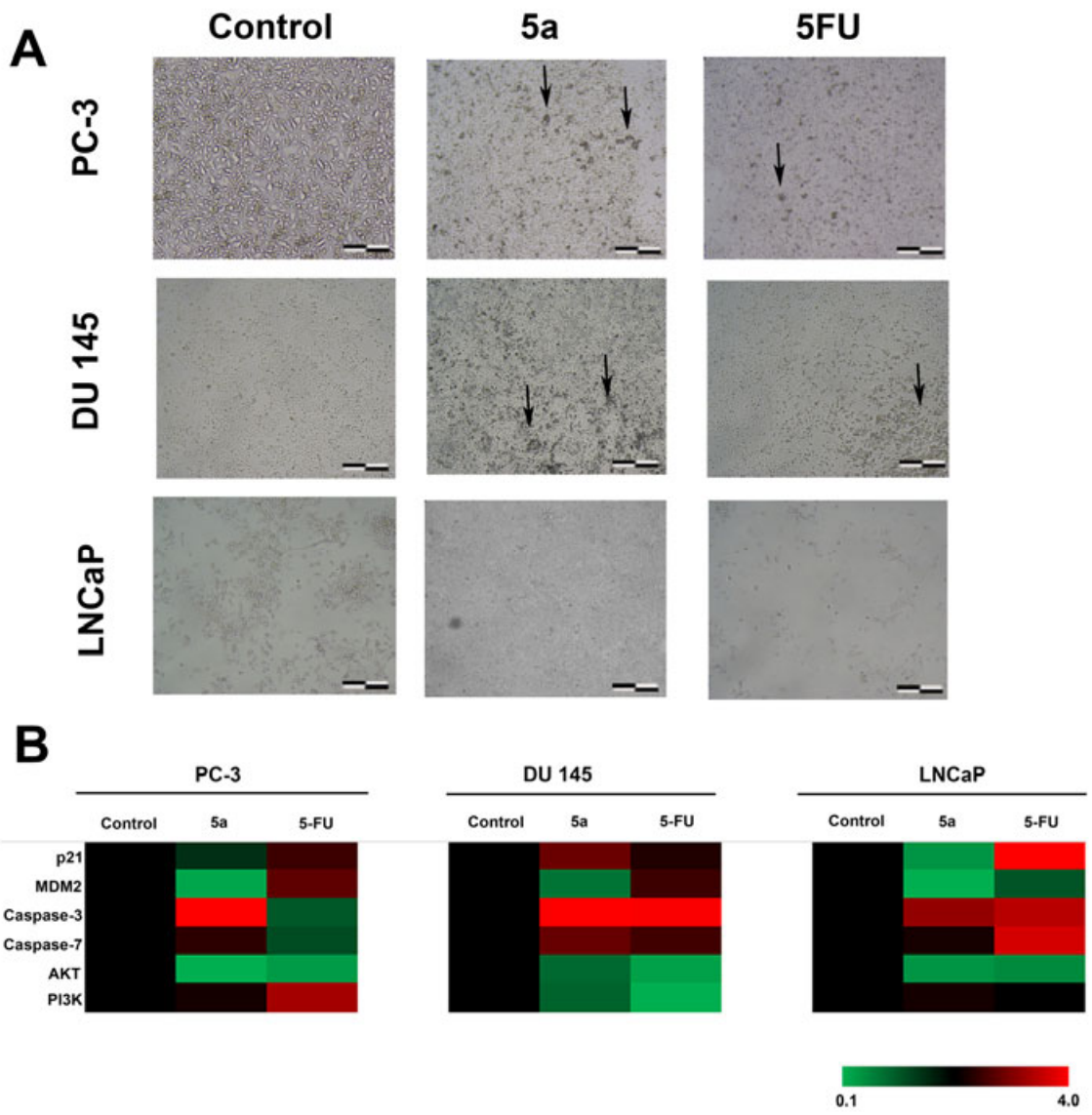

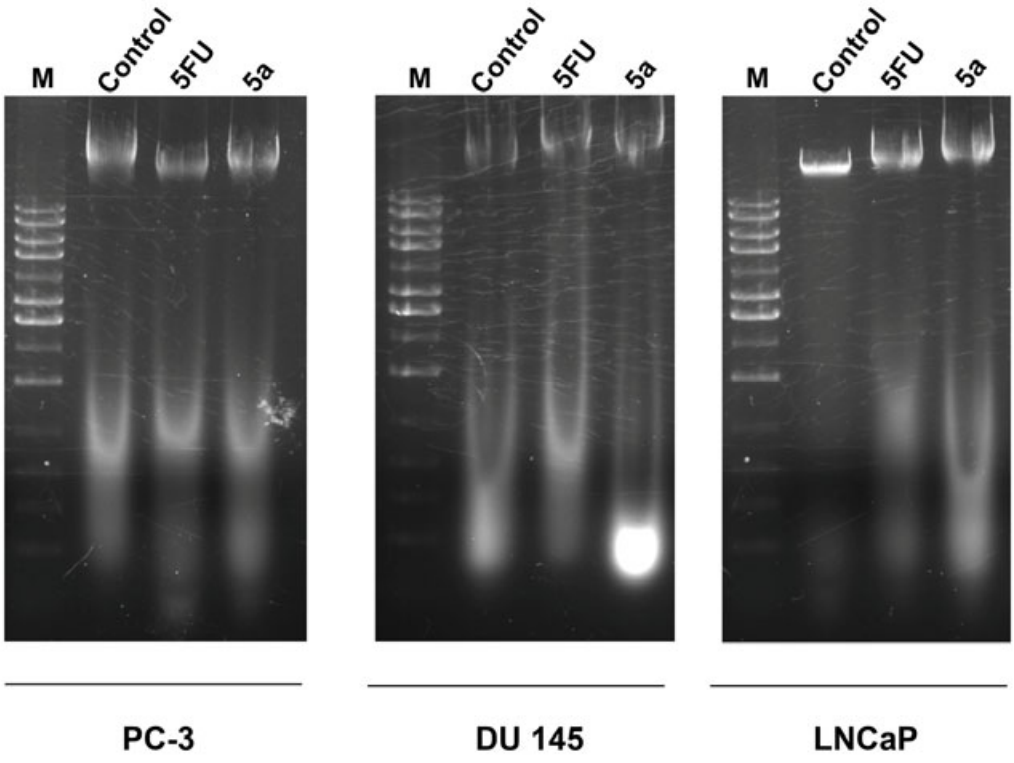

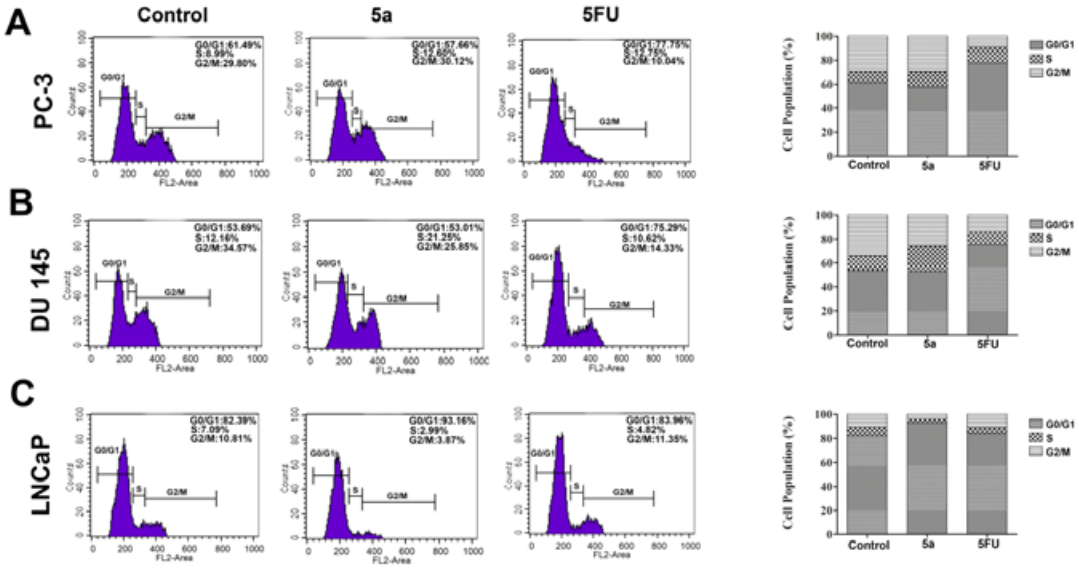

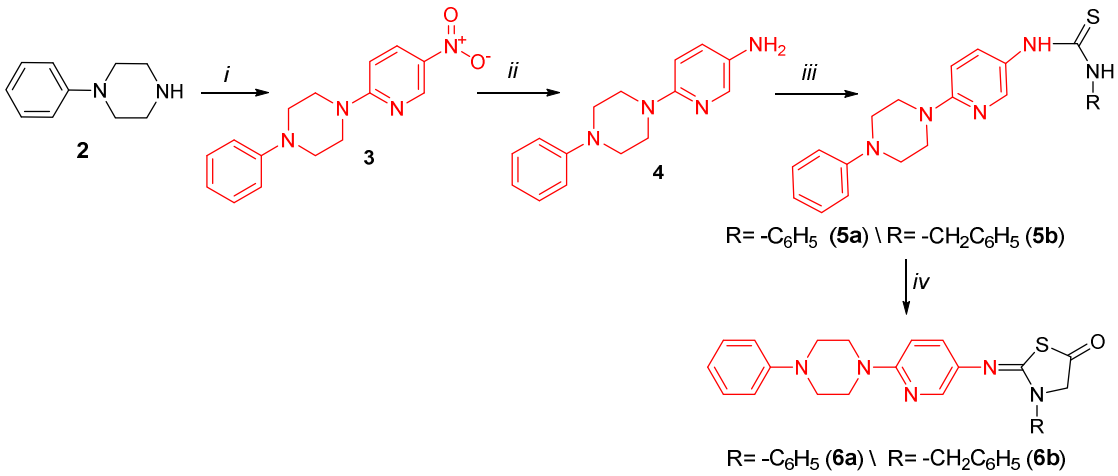

Scheme 1. The synthetic route of key intermediates 3-6[a]